

Mass enhancement of two-dimensional electrons in thin-oxide Si-MOSFET's

W. Pan and D. C. Tsui

Department of Electrical Engineering, Princeton University, Princeton, New Jersey 08544

B. L. Draper

Sandia National Laboratories, Albuquerque, New Mexico 87185

(May 20, 2018)

We wish to report in this paper a study of the effective mass (m^*) in thin-oxide Si-metal-oxide-semiconductor field-effect-transistors, using the temperature dependence of the Shubnikov-de Haas (SdH) effect and following the methodology developed by J.L. Smith and P.J. Stiles, Phys. Rev. Lett. **29**, 102 (1972). We find that in the thin oxide limit, when the oxide thickness d_{ox} is smaller than the average two-dimensional electron-electron separation r , m^* is still enhanced and the enhancement can be described by $m^*/m_B = 0.815 + 0.23(r/d_{ox})$, where $m_B = 0.195m_e$ is the bulk electron mass, m_e the free electron mass. At $n_s = 6 \times 10^{11}/\text{cm}^2$, for example, $m^* \simeq 0.25m_e$, an enhancement doubles that previously reported by Smith and Stiles. Our result shows that the interaction between electrons in the semiconductor and the neutralizing positive charges on the metallic gate electrode is important for mass enhancement. We also studied the magnetic-field orientation dependence of the SdH effect and deduced a value of 3.0 ± 0.5 for the effective g factor in our thin oxide samples.

Over two and a half decades ago, Smith and Stiles [1] reported their observation of effective-mass enhancement in the two-dimensional electron system (2DES) in silicon metal-oxide-semiconductor field-effect transistors (Si-MOSFET's). Following an earlier experiment by Fang and Stiles [2] on effective g factor enhancement, they were able to take advantage of the continuous density tunability of the device and carefully investigated the 2D electron density dependence of mass enhancement. Their finding that the effective mass m^* , in the unit of free electron mass m_e , continuously increases from ~ 0.21 to 0.225 for electron density (n_s) decreasing from $\sim 3 \times 10^{12}/\text{cm}^2$ to $0.6 \times 10^{12}/\text{cm}^2$ demonstrates unambiguously the electron-electron ($e-e$) interaction origin of the enhancement. Their experimental result was soon confirmed by theory and stimulated a great deal of theoretical interest in many-body effects in low dimensional electron systems. Subsequently, Fang, Fowler, and Hartstein [3] also investigated the influence of oxide charge and interface states on effective-mass measurement.

One question that was not addressed in these pioneering works is how the oxide thickness influences the mass enhancement. In particular, as the oxide thickness decreases, screening of the $e-e$ interaction by the metallic gate will become important. In the limit when the average $e-e$ separation is larger than the oxide thickness and the gate screening prevails, the $e-e$ interaction induced mass enhancement can be expected to diminish. In other words, if there is no other mechanism for enhancement, the mass as a function of n_s should show a decrease with decreasing n_s in this low density limit.

We wish to report in this paper a study of the effective mass in thin-oxide Si-MOSFET's, using the temperature dependence of the Shubnikov-de Haas (SdH) effect and following the methodology developed by Smith and Stiles [1]. We find that in the low-density limit,

when the oxide thickness d_{ox} is smaller than the average 2D $e-e$ separation r , defined by $r = 1/\sqrt{n_s}$, m^* is still enhanced and the enhancement can be described by $m^*/m_B = 0.815 + 0.23(r/d_{ox})$, where m_B is the bulk electron mass equal to $0.195m_e$. At $n_s = 0.6 \times 10^{12}/\text{cm}^2$, for example, $m^* = 0.25m_e$, an enhancement doubles that previously reported by Smith and Stiles. We also studied the magnetic-field orientation dependence of the SdH effect and deduced a value of 3.0 ± 0.5 for the effective g factor in our thin oxide samples.

The samples are n -type inverted silicon(100) surfaces on p -type substrates with peak mobility $1700 \text{ cm}^2/\text{V s}$ at 4.2 K. The thickness of the oxide (d_{ox}) is 60 Å. The channel length (L) is $2 \mu\text{m}$ and the channel width (W) $12 \mu\text{m}$. Since $W/L \gg 1$, the edge effect is not important in our experiments. The leakage current between the gate and the channel is virtually zero and much smaller than the drain-to-source current (I_{DS}). A drain voltage (V_D) not larger than $20 \mu\text{V}$ is applied throughout the experiment to ensure that the measurements are done in the Ohmic regime and there is no hot-electron effect. Transconductance, $G_m = dI_{DS}/dV_G$, is measured at a fixed magnetic field (here V_G is the gate voltage). The magnetic field (B) is chosen according to the following: (1) It has to be small enough so that the experiment is done in the SdH oscillation regime. (2) The B field has to be sufficiently large so that the SdH oscillations are clearly observed. The experiments are performed in a ^3He system, with a base temperature (T) of 0.3 K. The temperature uncertainty generally is smaller than ± 0.005 K. The measurements are done by employing a standard low-frequency lock-in technique, typically at 7 Hz. The results are reproducible from run to run after the same cool down. As many as ten samples of the same type are studied. All the samples give the same results within our experimental error.

In Fig. 1, we plot G_m as a function of V_G for one of the samples (sample A). The SdH oscillations are observed in electron densities down to $0.6 \times 10^{12}/\text{cm}^2$. G_m has been measured at many temperatures, and here three different temperature traces are shown to illustrate the temperature dependence of the oscillation amplitude. After the nonoscillatory background is subtracted, the oscillations are found to be sinusoidal with a single period, which proves that all electrons occupy one subband. The period of the oscillations is the change in V_G which produces a change in n_s equal to the number of electrons needed to fill a Landau level. This number is $4eB/h$ (here, e is the electronic charge, h is Planck's constant). Consequently, the minima in G_m vs. V_G occur whenever V_G satisfies

$$V_G = N(4e^2/hC_{ox})B + V_{th}, \quad (1)$$

where V_{th} is the threshold voltage, C_{ox} is the oxide capacitance, and N is an integer. Thus, if we label the minima (maxima) in G_m vs V_G from left to right by integer (half-integer) number N , a plot of N against V_G at which the minima (maxima) occur should yield a straight line. The inset of Fig. 1 shows such a plot, where the filled dots are the minima of the oscillations and the open dots the maxima. It is clear that the data points lie on a straight line and N follows a strictly linear dependence on V_G . The rate of change of n_s with respect to V_G , i.e., $dn_s/dV_G = C_{ox}/e$, obtained from the slope of the straight line is $3.4 \times 10^{12}/\text{cm}^2 \text{ V}$, in good agreement with that calculated from the oxide thickness. The intercept with the x axis at $N = 0$ gives $V_{th} = 0.57 \text{ V}$ for this sample.

The SdH formalism is used to derive the effective mass [1]. The absolute amplitude (A) of the SdH oscillations is obtained by subtracting the non-oscillatory background and drawing the envelope on the oscillatory part of the G_m traces. At each V_G , a set of amplitudes is then obtained from a set of temperature dependence data. The amplitude is fitted by a non-linear least-squares technique according to the equation

$$A \sim \frac{\xi}{\sinh(\xi)}, \quad (2)$$

where $\xi = 2\pi^2 k_B T / \hbar \omega_c = 2\pi^2 k_B T m^* / e \hbar B$, ω_c is cyclotron frequency, and m^* is the effective mass. All other symbols have their usual meanings. In the fitting, it has been assumed that the relaxation time τ is independent of temperature [1].

In Fig. 2(a), a plot of m^* vs n_s is shown for two samples. The solid symbols represent the results from sample A, and the open ones from sample B [4]. The effective mass shows an unexpectedly strong increase at low densities, up to $0.25m_e$ at $0.6 \times 10^{12}/\text{cm}^2$, even larger than what was reported by Smith and Stiles ($0.225m_e$ at the same density) [1], which is shown as the dashed line. The data cover the density range from $0.6 \times 10^{12}/\text{cm}^2$ to $2.0 \times 10^{12}/\text{cm}^2$, corresponding to an average $e - e$ separation varying from $r = 130 \text{ \AA}$ to 70 \AA . For $n_s <$

$0.6 \times 10^{12}/\text{cm}^2$, the absolute amplitude of the SdH oscillations is quite small while the nonoscillatory background is relatively large and steep. This fact makes the determination of the oscillation amplitude and the data fitting unreliable.

As we have mentioned above, in a thin-oxide Si-MOSFET, the effective mass is expected to decrease with decreasing density in the low electron density limit where the screening of the $e - e$ interaction by the metallic gate prevails. The observed strong mass enhancement, therefore, must originate from another mechanism, which becomes important in the low n_s limit. First, we want to point out that unavoidable charges in the oxide can not be the origin. The electron mass is known to show an opposite n_s dependence when a high concentration of charges is incorporated in the oxide [3]. Also, we recall that a MOSFET is simply a capacitor with the metallic gate and the semiconductor its two plates. The application of a gate voltage changes the amount of charge on the capacitor plates. With a positive V_G applied, electrons are transferred from the metallic gate electrode onto the silicon and are stored in the 2DES at the silicon surface. The metallic gate electrode, in turn, attains a sheet of positive charges, which can be conveniently viewed as mobile holes. Their influence on the dynamics of the 2DES is through the Coulomb screening [5], the strength of which is controlled by r/d_{ox} . In Fig. 2(b), m^* is replotted as a function of r/d_{ox} . We find that m^* shows a linear dependence on r/d_{ox} . In fact, within experimental error, all our data can be fitted by $m^*/m_B = 0.815 + 0.23(r/d_{ox})$. This empirical fit obviously breaks down in the $r \ll d_{ox}$ limit, where m^* is known to equal the bulk band mass $m_B = 0.195m_e$. In the $r/d_{ox} \rightarrow \infty$ limit, binding of the 2D electrons and the neutralizing holes on the metallic gate electrode is expected to form a 2D dipole gas and m^* , then, should be the mass of the electric dipole.

The mass enhancement due to the presence of the mobile holes on the gate electrode can be viewed as resulting from the Coulomb drag effect [6–9] — an interlayer Coulomb coupling between the electron layer in the semiconductor and the hole layer on the metallic gate electrode. In such a two layer system, when a current is driven through the electron layer, the interlayer $e - h$ interaction creates a frictional drag force that can modify the electron self-energy and change the effective mass. Several recent experiments [7–9] measured the interlayer scattering rate in bilayer parallel electron and parallel hole systems. Sivan, Soloman, and Shtrikman [9] studied the bilayer $e - h$ system in a GaAs/ $\text{Al}_{1-x}\text{Ga}_x\text{As}$ heterostructure and found that the scattering rate increases with decreasing n_s , similar to the n_s dependence of the mass enhancement observed in our experiment.

The magnetic-field orientation (θ) dependence of the SdH effect is also studied, from which an effective g factor is deduced by the coincidence method developed by Fang and Stiles [2]. Figure 3 shows two G_m traces at different tilt angles, $\theta = 0^\circ$ and $\theta = 68.0^\circ$. The total B

field is different for the two cases ($B = 3.75$ and 10.0 T respectively), but the perpendicular B field ($B_{\perp} = 3.75$ T) is kept the same. The phase of the two traces is roughly 180° different, or reversed [11]. For example, the minimum at $V_G = 1.02$ V in the $\theta = 0^{\circ}$ trace becomes a maximum in the $\theta = 68.0^{\circ}$ trace. The phase reversal can be understood from the fact that, while the Landau level separation ($\hbar\omega_c$) depends only on B_{\perp} , the spin splitting ($g\mu_B B$) depends on the total B field. As illustrated in the inset of Fig. 3, at $\theta = 0^{\circ}$, two spin-degenerate N th, $(N+1)$ th Landau levels give rise to the maxima at $V_G = 0.96$ and 1.09 V. By increasing θ , the spin degeneracy of Landau levels is lifted. The spin-up N th Landau level goes up while the spin-down $(N+1)$ th Landau level moves down. At $\theta = 68.0^{\circ}$, $g\mu_B B = \hbar\omega_c$ and the two levels cross to form the spin-degenerate Landau level giving rise to the maximum at $V_G = 1.02$ V. The effective g factor can be estimated from $g\mu_B B = \hbar\omega_c$ and we found for our samples $g = 3.0 \pm 0.5$. The large error bar is mainly due to the large Landau-level broadening and nonzero spin splitting at zero angle. Within this large experimental error, g factor shows no density dependence. Finally, similar large g factor enhancement was observed by Van Campen [10] who studied the magnetoconductance in high- B fields where the spin splitting is resolved. By fitting the line width of the magnetoconductance oscillations, he obtained a g factor from 2.5 to 3.6 at different densities in his sample with $d_{ox} = 44$ Å and peak mobility 6300 cm²/V s.

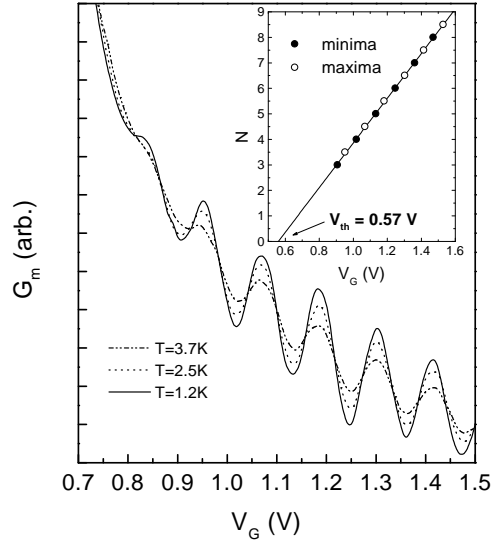
In conclusion, we have observed an unexpected mass enhancement in the low-density limit in thin-oxide Si-MOSFET's. The enhancement is attributed to the presence of the positive neutralizing charges on the metallic gate electrode at a distance smaller than the average $e-e$ separation. The effective g factor is also measured. Its value, 3.0 ± 0.5 , is larger than the bulk value and shows no dependence on the electron density within our experimental resolution.

We acknowledge help from J.P Lu and useful discussions with Harry Weaver and Kun Yang. The work done at Sandia was supported by the U.S. Dept. of Energy (DOE). Sandia National Laboratories is operated for DOE by Sandia Corporation, a Lockheed Martin Company, under Contract No. DE-AC04-94AL85000. The work at Princeton University was supported by the NSF.

smaller. The trend is real.

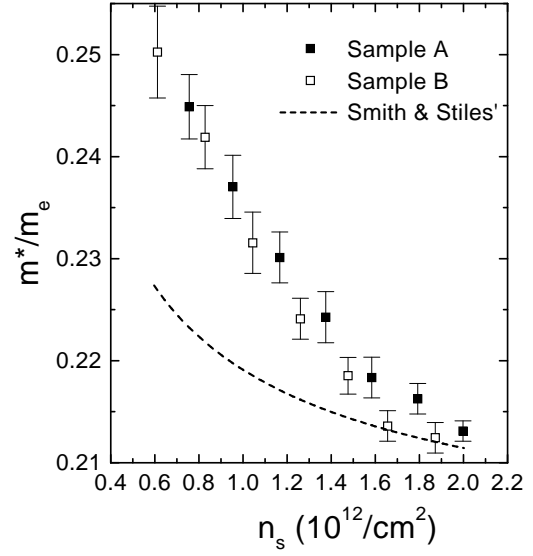
- [5] T. Ando, A.B Fowler and F. Stern, Rev. Mod. Phys. **54**, 437 (1982).
- [6] P.J. Price, Physica B **117**, 750 (1983).
- [7] P.M. Solomon, P.J. Price, D.J. Frank, and D.C.La Tulipe, Phys. Rev. Lett. **63**, 2508 (1989).
- [8] T.J. Gramila, J.P. Eisenstein, A.H. MacDonald, L.N. Pfeiffer, and K.W. West, Phys. Rev. Lett. **66**, 1216 (1991).
- [9] U. Sivan, P.M. Solomon, and H. Shtrikman, Phys. Rev. Lett. **68**, 1196 (1992).
- [10] S.D. van Campen, Ph.D. thesis, Lehigh University, 1994.
- [11] The period of SdH oscillations differs by approximately 10-15 % at the two angles in Fig. 3. There are several sources contributing to the difference. The first and the most important one is the uncertainty of the tilted angle, about 2° from the uncontrollable backlash of the gear in our probe. The second is due to the large Landau-level broadening and nonzero spin splitting at zero angle in our samples, which is also responsible for the large error bar in the g factor. Under this circumstance, the maxima of the SdH oscillations do not necessarily occur exactly at $g\mu_B B = \hbar\omega_c$. Instead, they can happen in a certain range of tilted angle. Finally, deformation of the electron wave function due to the large in-plane B field may also change the oscillation period for the two tilted angles with the same perpendicular B field.

-
- [1] J.L. Smith and P.J. Stiles, Phys. Rev. Lett. **29**, 102 (1972)
 - [2] F.F. Fang and P.J. Stiles, Phys. Rev. **174**, 823 (1968).
 - [3] F.F. Fang, A.B. Fowler, and A. Hartstein, Phys. Rev. B **16**, 4446 (1977).
 - [4] The error bar represents one standard statistical deviation from data fitting. The error at higher density is

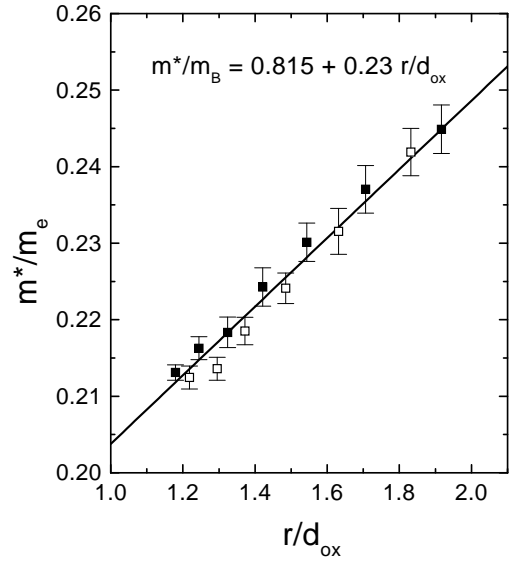


Pan et al/ Fig. 1

FIG. 1. The temperature dependence of G_m for sample A. Three temperature traces are shown at $T = 1.2, 2.5, 3.7$ K. The inset shows N vs V_G at which the minima (maxima) of G_m occur. The close dots are the minima, the open ones the maxima. The straight line is a linear fit to the data. V_{th} is the threshold voltage.

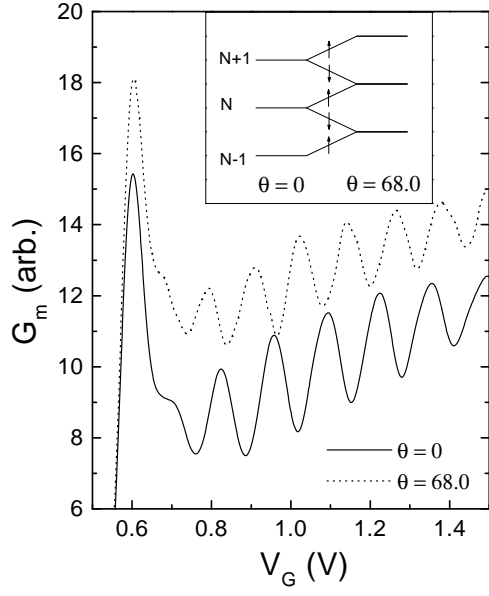


Pan et al/ Fig. 2a



Pan et al/ Fig. 2b

FIG. 2. (a) m^* vs n_s for two samples, sample A (the solid symbols) and sample B (the open symbols). The dash line represents the previous result from Smith and Stiles. (b) The replot of m^* as a function of r/d_{ox} . m^* shows a linear dependence on r/d_{ox} .



Pan et al/ Fig. 3

FIG. 3. G_m vs V_G for $B = 3.75$ T at $\theta = 0^\circ$ and $B = 10.0$ T at $\theta = 68.0^\circ$. B_\perp is the same for the two cases. The upper trace is shifted vertically by a factor of 3 units. The phase reversal is clearly seen for the two traces. The inset shows the evolution of Landau levels with the tilt angle.